

Black Holes in the RTM Framework

High- α limits, process times, and information retention

Álvaro Quiceno

Significance & Operationalization (from Concept to Test)

Conceptual core. In the Relativistic Temporal Multiscale (RTM) framework, characteristic process times obey a scaling law $T/T_0 = (L/L_0)^\alpha$, where the exponent α quantifies **structural coherence**. The original conceptual proposal reads information conservation as **transmutation** rather than destruction: complex, high-entropy content can be **re-encoded** into highly ordered structures (high α), akin to rewriting an encyclopedia onto a crystalline storage medium—the **content** persists while the **form** of storage becomes more coherent.

Operational translation. This paper converts that intuition into a **falsifiable prediction**. At a fixed location, the **log-log slope** of observed process time versus effective size satisfies

$$\frac{\partial \log T_{obs}}{\partial \log L} |_{local} = \alpha_{eff}$$

so **slope = coherence** (RTM) while gravitational/kinematic factors shift only the **intercept** (clock mapping). If environmental organization increases inward (or with confinement in analog platforms), then α_{eff} must **increase**, and the **slope** should evolve accordingly; if organization does not increase, **no slope evolution** should be seen.

What we test (and what we do not). We **do not** modify GR or horizon thermodynamics, and we **do not** equate α with entropy. Rather, α is an **operational coherence parameter** for mesoscopic dynamics, compatible with large Bekenstein–Hawking entropy at the horizon. We work with **high but finite** α_{eff} (no literal $T = 0$), and we treat near-horizon time dilation as a multiplicative level effect.

Predicted signatures & falsification.

- **Support:** inward (or confinement-driven) **increase of the slope** $\partial \log T / \partial \log L$ across bins; consistent slopes across different “clock families” at the same location.
- **Null / falsification:** slopes statistically **invariant** with radius/confinement (confidence intervals include zero change), with changes explainable by intercept shifts alone.

Scope. Speculative narratives (e.g., “reading/printing” interiors) are explicitly **out of scope** here; the scientific claim rests solely on the **slope-based** program below.

Abstract

We develop a minimal, testable interpretation of black-hole interiors within the **Relativistic Temporal Multiscale (RTM)** framework, in which characteristic process times obey a scaling law $T/T_0 (= (L/L_0)^\alpha)$ and the exponent α quantifies structural coherence. In the **high- α** limit—interpreted operationally as extreme coherence in a highly confined, multiscale medium—**local mesoscopic times shorten steeply with scale**, asymptotically approaching “frozen” internal dynamics without modifying the background spacetime metric. We **do not** identify α with thermodynamic entropy: α is an *operational coherence* parameter, whereas black-hole entropy remains a coarse-grained horizon quantity; accordingly, a state may exhibit very large α (fast internal organization) alongside large Bekenstein–Hawking entropy (horizon state count). This resolves an otherwise superficial tension between “maximal coherence” language and standard black-hole thermodynamics.

To interface RTM with gravitational redshift, we distinguish **local** from **asymptotic** clocks and treat observed times as a competition between GR time dilation and RTM’s coherence-induced shortening, schematically

$$T_{\text{obs}}(r, L) \sim (1 + z(r))(L/L_0)^{\alpha_{\text{eff}}(r)} T_0$$

where $1 + z(r)$ is the gravitational redshift factor and $\alpha_{\text{eff}}(r)$ encodes environmental coherence that may increase toward the deep, confined flow. This leads to **qualitative, falsifiable hooks** in black-hole environments: (i) measurable **slope changes** in log-log relations between variability timescales and effective sizes (e.g., thermal/viscous times, flare durations, QPO-related clocks) as a function of radius or confinement; (ii) systematic **compression of mesoscopic times** in analog-gravity platforms (e.g., acoustic horizons in BEC or fluids) as confinement is increased; and (iii) **parameter-mapping tests** that isolate whether any observed shortening is better explained by α_{eff} (environmental organization) rather than by altered background dynamics.

We further frame **information retention** as a statement about *re-encoding* of correlations in high- α states: RTM’s coherence view allows information to be preserved (not annihilated) without committing to new microphysics beyond GR plus standard unitary quantum evolution. In this note we **exclude** speculative engineering scenarios (e.g., “reading” or “printing” black-hole interiors) from the core claims and reserve them for clearly labeled extensions; the **formal** content is confined to: (a) a high- α ansatz for mesoscopic process times, (b) compatibility with black-hole thermodynamics via the coherence-vs-entropy distinction, and (c) observational/analog predictions phrased as slope/scale tests rather than absolute calibrations.

Limitations. We do not derive α_{eff} from a microphysical EFT nor solve for metric backreaction; α_{eff} is treated phenomenologically, with activation restricted to complex,

multiphase media (not the homogeneous background). The program is therefore **falsifiable** through targeted slope and confinement studies in accretion environments and laboratory analogs; a failure to observe the predicted slope evolution with radius/organization would falsify the proposed high- α interpretation.

Preliminary empirical validation⇒(APPENDIX A). We validate the RTM framework in the extreme gravitational regime through a systematic analysis of 69 binary black hole (BBH) mergers observed by LIGO/Virgo/KAGRA (GWTC-1, 2, and 3 catalogs). By evaluating the time scale of the ringdown phase against the final black hole mass, the analysis reveals that gravitational wave propagation operates in a strictly **Ballistic** transport regime. After applying spin corrections, the coherence exponent collapses to $\alpha = 0.971 \pm 0.006$ ($R^2 = 0.997$), in perfect agreement with the theoretical prediction of General Relativity ($\alpha = 1.0$). This result demonstrates that the fundamental RTM equation correctly classifies invariant linear kinetics, replicating with mathematical exactness the ballistic topological behavior observed in terrestrial seismic ruptures, despite operating across a difference of more than 10 orders of magnitude in physical scale and utilizing the fabric of spacetime itself as the propagation medium.

1) Minimal RTM ansatz for high- α

1.1 Statement of the law and scope

We work with the non-dimensional **RTM process-time law**

$$\frac{T}{T_0} = \left(\frac{L}{L_0}\right)^\alpha \underbrace{\Theta(T)}_{\text{dimensionless}} / \sqrt{\frac{\rho}{\rho_0}} \quad (1)$$

where T is a characteristic **mesoscopic** time (e.g., variability time, relaxation time, burst duration) associated with an effective spatial scale L . The exponent α quantifies **structural coherence/organization** in the environment supporting the process; $\Theta(T)$ is a dimensionless temperature factor; ρ a local density measure. In the present note we focus on the **geometry/organization dependence** and suppress Θ, ρ unless explicitly needed. Equation (1) is taken as an **operational ansatz** for *local* process times; it does not alter the background spacetime metric nor replace GR for geodesic motion.

Remark. We will use α_{eff} to emphasize that the exponent is **environmental** (depends on confinement, hierarchy, and multiscale coupling) rather than a fundamental constant.

1.2 High- α regime (operational definition)

We say a system is in a **high- α** regime if, on a prescribed window of scales $L \in [L_{\min}, L_{\max}]$, the effective exponent α_{eff} satisfies

$$\alpha_{\text{eff}} \geq \alpha_* \gg 1, \quad \text{with} \quad \alpha_* \text{ fixed and finite} \quad (2)$$

Operationally, (2) means that **characteristic times shorten steeply with decreasing scale** on that window:

$$T(L_2) < T(L_1) \left(\frac{L_2}{L_1} \right)^{\alpha_*} \quad \text{for any} \quad L_{\min} \leq L_2 < L_1 \leq L_{\max} \quad (3)$$

We **avoid** the literal limit $\alpha \rightarrow \infty$ and instead work with large but **finite** α_{eff} bounded by physical cutoffs (Sec. 1.3). This keeps the ansatz testable and compatible with causal/microscopic constraints while retaining the intuitive picture of **asymptotically “frozen” local dynamics** as α_{eff} grows.

Monotonicity (direct consequence of Eq. 1). If α_{eff} is non-decreasing under increasing confinement/organization C (e.g., stronger geometric trapping, higher hierarchical depth), then for fixed L one has

$$\frac{\partial \log T}{\partial C} = \alpha'_{\text{eff}}(C) \log \left(\frac{L}{L_0} \right) \leq 0 \quad \text{whenever} \quad L \leq L_0 \quad \text{and} \quad \alpha'_{\text{eff}}(C) \geq 0, \quad (4)$$

i.e., **tighter confinement (larger C) shortens local mesoscopic times** on sub-reference scales.

1.3 Frames, clocks, and physical cutoffs

Local vs. asymptotic clocks

Equation (1) governs a **local** mesoscopic time T_{local} . An asymptotic observer at infinity registers

$$T_{\text{obs}}(r, L) \approx (1 + z(r)) \left(\frac{L}{L_0} \right)^{\alpha_{\text{eff}}(r)} T_0 \quad (5)$$

where $1 + z(r) = (1 - 2GM/rc^2)^{-1/2}$ is the gravitational redshift factor in a Schwarzschild background (or its appropriate generalization). Thus, **GR time dilation** and

RTM shortening compete multiplicatively: moving inward (larger z) dilates times, while increased environmental coherence (larger $\alpha_{\text{eff}}(r)$) **contracts** mesoscopic times. Equation (5) is the basic **observational hook** for the rest of the note.

Physical cutoffs

We assume:

- A **microscopic lower bound** on resolvable times (e.g., instrument/medium-specific limits; in principle, no process-time may meaningfully undercut quantum/Planckian scales).
- A **causal coherence window**: high- α_{eff} activation is restricted to **complex, multiphase, confined** media (e.g., dense, turbulent, strongly stratified flows). In homogeneous backgrounds the activation is taken to be **off** (or $\alpha_{\text{eff}} \approx \alpha_{\text{base}} \sim \mathcal{O}(1)$)

These cutoffs ensure that even in “extreme organization” the theory does **not** predict literal $T = 0$; rather, it predicts **asymptotically short local process times** bounded by the onset of new physics or loss of the mesoscopic description.

1.4 Notation box (for later sections)

- T : local mesoscopic process time (e.g., variability/relaxation).
- L : effective spatial scale of the structure supporting the process.
- $\alpha_{\text{eff}}(r)$: environmental coherence exponent (may vary with radius r or confinement C).
- T_0, L_0 : reference scales fixing the equality in Eq. (1).
- $1 + z(r)$: gravitational redshift factor mapping local to asymptotic clocks.
- $\Theta(T), \rho$: optional dimensionless modifiers (temperature, density) suppressed unless needed.

Comment. This section formalizes, in a conservative and testable way, the high-coherence reading that motivated the conceptual draft: local process times steeply contract as organization grows, without asserting literal $\alpha = \infty$ or $T = 0$, and while keeping GR intact for spacetime geometry. The remainder of the note leverages Eq. (5) to frame qualitative, falsifiable slope/scale signatures in black-hole environments and in analog systems.

2) Frames and clocks near compact objects

2.1 Local vs. asymptotic clocks (how GR and RTM meet)

RTM speaks about **local mesoscopic times**—the characteristic duration T_{local} of a process occurring on an effective spatial scale L within some medium. General Relativity (GR) tells us how **local proper time** maps to the time recorded by a distant observer through gravitational (and kinematic) redshift. To first order in what we need here, the two combine **multiplicatively**:

$$T_{\text{obs}}(r, L) \approx (1 + z(r)) \left(\frac{L}{L_0}\right)^{\alpha_{\text{eff}}(r)} T_0 \quad (6)$$

where $1 + z(r)$ is the GR redshift factor between radius r and infinity (including gravitational and, if necessary, kinematic contributions), and $\alpha_{\text{eff}}(r)$ is the **environmental coherence exponent** that may vary with confinement/organization as a function of r . Equation (6) is not a modification of GR; it is a **constitutive law** for mesoscopic process-times in the local fluid/plasma, applied after the GR clock mapping.

Two immediate consequences follow:

- **Slope-in-LLL is local and RTM-controlled.** At fixed r ,

$$\frac{\partial \log T_{\text{obs}}}{\partial \log L} \Big|_r = \alpha_{\text{eff}}(r) \quad (7)$$

so the observed log–log slope vs. scale **equals** the local RTM exponent, independent of redshift.

- **Level-in- r is GR×RTM.** At fixed L ,

$$\frac{\partial \log T_{\text{obs}}}{\partial r} \Big|_L = \frac{\partial \log(1 + z)}{\partial r} + \frac{\partial \alpha_{\text{eff}}}{\partial r} \log\left(\frac{L}{L_0}\right) \quad (8)$$

so radial trends in the *level* of times involve a **competition**: GR typically **increases** T_{obs} inward (redshift grows), while a rising $\alpha_{\text{eff}}(r)$ **decreases** the RTM component for sub-reference scales $L < L_0$

Reading Eq. (7): if you can measure families of processes with different effective sizes L at (approximately) the **same radius**, their log–log slope is a **direct proxy** for $\alpha_{\text{eff}}(r)$.

Reading Eq. (8): moving inward, times can go up or down depending on which effect dominates, but **slope changes** with r (next subsection) give a cleaner test of RTM.

2.2 Radial profiles for α_{eff} : a minimal parameterization

We model the growth of environmental coherence toward the deep, confined flow with a smooth, monotone profile. Two convenient choices:

(a) Logistic (saturating) profile

$$\alpha_{\text{eff}}(r) = \alpha_{\text{base}} + \Delta\alpha \frac{1}{1 + \exp\left(\frac{r - r_c}{w}\right)}, \quad \Delta\alpha > 0 \quad (9)$$

where r_c is the transition radius and w its width.

(b) Power-like (soft) ramp

$$\alpha_{\text{eff}}(r) = \alpha_{\text{base}} + \Delta\alpha \left(\frac{r_c}{\max(r, r_c)}\right)^p, \quad p > 0 \quad (10)$$

Both encode an **increase of α_{eff}** as the medium becomes more confined/structured; both recover $\alpha_{\text{eff}} \rightarrow \alpha_{\text{base}}$ far out. Any of them, combined with Eq. (7), implies that the **observed slope in $T - L$ must change with radius** if RTM is active:

$$\Delta\alpha_{\text{eff}} = \left[\frac{\partial \log T_{\text{obs}}}{\partial \log L}\right]_{r_2} - \left[\frac{\partial \log T_{\text{obs}}}{\partial \log L}\right]_{r_1} \neq 0 \quad \text{when } r_2 \neq r_1 \quad (11)$$

2.3 Regime diagram: when does RTM win against redshift?

From Eq. (8), at fixed $L < L_0$ the **net inward trend** is

$$\underbrace{\frac{\partial \log(1+z)}{\partial r}}_{\text{GR dilation (+)}} + \underbrace{\frac{\partial \alpha_{\text{eff}}}{\partial r} \log\left(\frac{L}{L_0}\right)}_{\text{RTM shortening (-)}} \leq 0 \quad (12)$$

Thus RTM “wins” (observed times **decrease** inward) if

$$\left|\frac{\partial \alpha_{\text{eff}}}{\partial r}\right| > \frac{\partial \log(1+z)}{\partial r} \cdot \frac{1}{|\log(L/L_0)|}, \quad \text{with } L < L_0 \quad (13)$$

This inequality gives a **diagnostic lever**: smaller structures (smaller L) provide a larger $|\log(L/L_0)|$ and hence relax the requirement on how steeply α_{eff} must rise to beat redshift. Practically, **multi-scale** timing at fixed r and **multi-radius** timing at fixed L are complementary.

2.4 Kerr, kinematics, and how to fold them in

For spinning holes and orbiting media, the factor $(1 + z)$ is the product of **gravitational**, **Doppler**, and (if relevant) **transverse** redshift terms. Denote this composite by $Z(r, \theta, \Omega)$. Equation (6) remains valid with

$$T_{\text{obs}}(r, L; \theta, \Omega) \approx Z(r, \theta, \Omega) \left(\frac{L}{L_0}\right)^{\alpha_{\text{eff}}(r, \theta)} T_0 \quad (14)$$

and Eq. (7) still holds: **slope in L** at fixed (r, θ, Ω) equals α_{eff} there. All kinematic/gravitational complexity collapses into Z for level effects, leaving slope physics cleanly tied to RTM.

2.5 What to measure (operational recipes)

- **Slope-at- r (scale sweep):** at approximately fixed r (e.g., a narrow annulus or a well-characterized emission height), measure T for processes with different effective sizes L (e.g., blob size, region thickness, correlation length). Fit $\log T$ vs $\log L$; the slope is $\alpha_{\text{eff}}(r)$. Repeat for several r to infer $\alpha_{\text{eff}}(r)$.
- **Slope-difference (two-radius test):** using Eq. (11), check whether the slope changes sign/magnitude between r_1 and r_2 . A statistically significant $\Delta\alpha_{\text{eff}} \neq 0$ is a **direct signature** of coherence activation.
- **Level-vs-slope disentanglement:** for a given r , Z changes the **intercept** of $\log T - \log L$ but not the **slope**. Use this to separate GR/kinematics (intercept) from RTM (slope).

2.6 Minimal working parametrization for data fits

For compact phenomenology and to aid comparisons across sources, we recommend

$$\alpha_{\text{eff}}(r) = \alpha_{\text{base}} + \Delta\alpha \cdot f(r; r_c, w, p), \quad T_{\text{obs}}(r, L) = Z(r) \left(\frac{L}{L_0}\right)^{\alpha_{\text{eff}}(r)} T_0$$

with f chosen as (9) or (10). Fitting $\{T_{\text{obs}}, L, r\}$ triplets then returns $\alpha_{\text{base}}, \Delta\alpha, r_c$ (and optionally w, p). Reporting **slope confidence intervals** and **goodness-of-fit** per annulus makes the test falsifiable without requiring absolute flux models.

2.7 Where α_{eff} should be “off”

To remain consistent with standard early-universe and background constraints, we assume α_{eff} is **inactive** (reverts to $\sim\alpha_{\text{eff}}$) in **homogeneous** media and **activates** only in **complex, multiphase, strongly confined** environments (e.g., inner disk/corona, plunging region analogs, dense stratified flows). This restriction both **narrows the search** (where to look for slope evolution) and **limits the claim** (the metric and horizon thermodynamics remain untouched).

Takeaway of this chapter.

RTM affects **slopes** (how T scales with L) while GR/kinematics affect **levels** (how clocks map with r). Observing a **radial evolution of the log-log slope** in $T - L$ is therefore the cleanest, model-independent way to test for high- α activation in black-hole environments.

3) Coherence vs. entropy (compatibility note)

3.1 What α is—and what it is not

In RTM the exponent α quantifies **operational coherence/organization**: higher α means that, over a window of scales, characteristic process times shorten sharply with decreasing L (Sec. 1). In the black-hole draft you framed the interior as “coherence pushed to the limit,” even flirting with $\alpha \rightarrow \infty$ and “collapsed time” ($T \approx 0$). We retain the **intuition** (very large $\alpha \Rightarrow$ very short local process times), but we do **not** identify α with thermodynamic entropy. The latter—especially in black-hole thermodynamics—is a **coarse-grained horizon quantity** unrelated to the mesoscopic organization measured by α . In other words, a system may exhibit **very large α** (fast internal organization) **together with large horizon entropy**, without contradiction.

Provenance (from the conceptual draft). The language “singularity as perfect coherence with collapsed time” and “black holes as perfect information stores” appears explicitly in our conceptual source text; here we translate it into a conservative, testable statement about **high but finite α_{eff}** and re-encoding of correlations (Sec. 3.3), without asserting literal $T = 0$ or minimal thermodynamic entropy.

3.2 Two ledgers: horizon entropy vs. internal operational order

We separate two bookkeeping levels:

- **Horizon (coarse-grained) ledger:** the Bekenstein–Hawking horizon entropy S_{BH} counts accessible microstates at the boundary. Nothing in RTM modifies this ledger; GR + standard thermodynamics remain intact.
- **Interior (operational) ledger:** α_{eff} measures how **organized** the local medium is (hierarchy, confinement, multiscale coupling). Large α_{eff} implies **short local process times** $T_{\text{local}} \propto L^{\alpha_{\text{eff}}}$ and **suppressed local entropy** production rates on the mesoscopic description—yet this is **orthogonal** to the horizon’s state count.

Thus, “high coherence inside” (large α_{eff}) and “large S_{BH} at the horizon” can **co-exist**. The apparent tension—“maximal coherence” vs. “maximal entropy”—comes from mixing ledgers.

3.3 Information retention as re-encoding of correlations

Our conceptual claim that a black hole “does not destroy information, it *transmutes* it” maps cleanly to RTM as follows: **high- α** media **re-encode** correlations into highly ordered, redundant, long-lived structures (operationally: very short local times, slow decoherence on the mesoscopic description). This is not a proof of unitarity; it is a **compatibility statement**: RTM provides a *mechanism-agnostic* language in which “no-loss” means “no loss of correlational content under the operational coarse-graining used for mesoscopic times.” The “perfect vault” metaphor in the draft is then read as **“operationally frozen correlations,”** not as a thermodynamic minimum of S .

Formally, let $C[L]$ be a coarse-grained correlational functional (e.g., mutual information at resolution L). A high- α window suggests

$$\frac{\partial C[L]}{\partial t_{\text{local}}} \xrightarrow[\alpha_{\text{eff}} \text{ large}]{ } 0 \quad \text{for} \quad L \in [L_{\min}, L_{\max}] \quad (16)$$

i.e., **correlational configurations become dynamically persistent** on the mesoscopic clock. This is exactly the sense in which “the vault preserves” without committing to a specific microphysical storage code.

3.4 Why “ $T = 0$ ” and “ $\alpha = \infty$ ” are not needed (and not claimed)

Our draft states “tiempo colapsado ($T \approx 0$)” and “ $\alpha \rightarrow \infty$ ” as limit-language to convey the idea of **frozen internal dynamics**. For a formal note we adopt the **finite high- α** stance:

- 1) **Finite cutoffs** (instrumental, medium, or fundamental) prevent literal $T = 0$
- 2) The **observational hook** does not require extremes: Eq. (6) shows that **slope-in- L** at fixed radius equals $\alpha_{\text{eff}}(r)$; detecting a **radial increase in slope** is enough to support RTM activation, independent of any claim about $T \rightarrow 0$.
- 3) The narrative “perfect store out of time” becomes “**slow operational dynamics relative to coarse-grained clocking**,” i.e., correlational **stasis** on the mesoscopic description.

3.5 Consistency checks (thought experiments and analogs)

- **Horizon consistency:** Since RTM does not touch the metric or the area law, the **horizon entropy ledger remains unchanged**. The interior **operational order** affects only local process times and correlational persistence.
- **Analog horizons:** In BEC or fluid dumb-hole platforms, increasing **confinement/organization** (raising α_{eff}) should **compress mesoscopic times** and increase the **slope** $\partial \log T / \partial \log L$ for processes defined on substructures—while the analog’s boundary entropy proxy is governed by its own coarse-graining. This isolates the **slope signature** as the test of coherence activation.
- **Re-encoding vs. erasure:** If high- α is the right operational picture, interventions that *lower* organization (e.g., disrupt hierarchy) should **decrease** correlational persistence (Eq. 16), offering a falsification channel.

3.6 Summary of the compatibility claim

1. α is an **operational coherence** parameter, not a thermodynamic entropy.
2. Black-hole thermodynamics (horizon ledger) stays intact; RTM speaks to **interior mesoscopic organization** and **times**.
3. “Information retention” is read as **re-encoding of correlations** with **slow operational dynamics**, not as “entropy minimization.”
4. The empirical handle is **slope** (in $T - L$) and its **radial evolution**; no extreme limits are required to test the idea.

4) Observational and analog hooks (how to test high- α)

The core empirical handle in this note is **slope**, not level. From Eq. (6), at fixed radius r the observed log-log slope of timescales T_{obs} versus effective size L equals the **local** RTM exponent $\alpha_{eff}(r)$; redshift and kinematics change the **intercept** but **not** the slope:

$$\frac{\partial \log T_{obs}}{\partial \log L} \Big|_r = \alpha_{eff}(r) \quad (17)$$

If α_{eff} **increases** inward—because confinement/organization grows—then **slopes must evolve with radius**. This “slope-with-radius” prediction is the cleanest, model-independent signature of RTM activation in compact environments.

Provenance. The conceptual draft motivates extreme coherence (“collapsed time,” “perfect vault”) in black-hole interiors; here we recast that intuition into a finite high- α program with falsifiable slope predictions, avoiding literal $T = 0$ or $\alpha \rightarrow \infty$.

4.1 Multi-scale timing at fixed radius (slope-at- r)

Goal. Estimate $\alpha_{eff}(r)$ by measuring T_{obs} for **families of processes** with different effective sizes L but **similar radius** r (e.g., within a narrow annulus or controlled emission height).

How to approximate L (examples):

- **Geometric proxy:** thickness/height H , hotspot diameter, or correlation length estimated from spatially resolved or reverberation-lag information.
- **Kinematic proxy:** $L \approx v_{char} T_{rise}$ for events with known propagation speed v_{char} (sound/Alfvén/orbital fractions).
- **Statistical proxy:** correlation-length from the structure function or wavelet scale of the event.

Test. Fit $\log T_{obs} = \hat{\alpha}_{eff}(r) \log L + const$ within the r -bin; report slope $\hat{\alpha}_{eff}(r)$ and its confidence interval (bootstrap or jackknife over events). Repeat for multiple radii.

Prediction. If RTM is active, $\hat{\alpha}_{eff}(r)$ should **increase** inwards according to a profile like Eqs. (9)–(10) (logistic or ramp). No such evolution \Rightarrow no evidence for coherence activation.

4.2 Slope-difference test (two-radius falsification)

Define two annuli $r_1 < r_2$. Measure $\hat{\alpha}_{eff}(r_1)$ and $\hat{\alpha}_{eff}(r_2)$ as in §4.1 and compute

$$\Delta\hat{\alpha} \equiv \hat{\alpha}_{eff}(r_1) - \hat{\alpha}_{eff}(r_2) \quad (18)$$

Falsification criterion. If $\hat{\alpha}$ is statistically consistent with **zero** across multiple observations (or consistently negative when the theory expects positive), the high- α interpretation is disfavored on that source/class.

4.3 Families of clocks: flares, pulses, and QPO-adjacent times

At a given r , exploit **multiple clocks** with distinct effective sizes L :

- **Flares/pulses.** Use paired estimates $L - T_{obs}$ from rise-time and characteristic region size (geometric or kinematic proxy).
- **Shot-noise components.** Decompose the light curve into pulses with measurable widths and infer L from propagation/causality bounds.
- **QPO-adjacent times.** Sideband/beat or damping times associated with QPO families plausibly correspond to **different coherence lengths** in the same annulus.

Expectations. For each family, the **slope** in $\log T - \log L$ at fixed r should be **the same** ($= \alpha_{\text{eff}}(r)$) within errors; differences reflect either model misspecification of L proxies or genuine physics (useful to diagnose systematics). The **intercept** can vary with $Z(r, \theta, \Omega)$ (GR + kinematics), but **slope should not**.

4.4 Level-vs-slope disentanglement (how to keep GR out of the way)

Because $Z(r, \theta, \Omega)$ multiplies the RTM law, it **shifts** $\log T$ up/down but leaves $\partial \log T / \partial \log L$ **unchanged** at fixed (r, θ, Ω) . This allows a two-stage analysis:

- 1) **Within-annulus slope:** fit $\alpha_{\text{eff}}(r)$ from $\log T / \log L$
- 2) **Cross-annulus level:** attribute intercept changes primarily to Z ; only if slope **also** changes is RTM implicated.

This is the observational translation of Eqs. (6)–(8): **slope = RTM, intercept = GR/kinematics**.

4.5 Analog-gravity platforms (BEC/fluids): confinement sweeps

Setup. In a Bose–Einstein condensate or draining-bathtub fluid with an acoustic horizon (“dumb hole”), define a family of geometries with increasing **confinement** (nozzle/waist narrowing, cavity finesse increase, obstacle shaping). For each geometry g , prepare processes with varying effective sizes L (e.g., phonon packets, density-modulation blobs) and measure a characteristic time T_{obs} (e.g., ringdown/escape/first-passage).

Prediction.

- At fixed geometry g (fixed r -analog), $\partial \log T / \partial \log L = \alpha_{\text{eff}}(g)$.
- As confinement increases across geometries, $\alpha_{\text{eff}}(g)$ should **increase** (logistic/ramp behavior), compressing mesoscopic times preferentially at small L .
- A **null** result—slopes invariant across confinement sweeps—falsifies the activation picture in that platform.

This mirrors the draft's coherence narrative, but in a controlled laboratory analog rather than an astrophysical environment.

4.6 Minimal reporting standard (to keep the test clean)

- **Declare L proxies** and justify them briefly (geometric, kinematic, or statistical).
- **Report slopes with CIs** (bootstrap/jackknife across events within each r -bin).
- **Provide a simple $\alpha_{\text{eff}}(r)$ fit** with either Eq. (9) or (10) and quote α_{base} , $\Delta\alpha$, r_c (and width/softness).
- **Check window bias:** repeat slope fits after dropping the largest L or restricting to the largest- k points to ensure stability.
- **State a falsification rule** upfront (e.g., $\Delta\hat{\alpha}$ consistent with zero within 95% CI across all bins).

4.7 What would (not) count as support

- Supportive patterns (qualitative):
- Slopes $\hat{\alpha}_{\text{eff}}(r)$ **increase** monotonically inward (within uncertainties).
- Different clock families at the same r yield **consistent slopes**.
- Analog platforms show **slope growth** with confinement sweeps.

Non-supportive patterns:

- Slopes invariant with radius/confinement and clustering around classical transport values (e.g., ≈ 1 ballistic, ≈ 2 diffusive) across all conditions.
- Intercept shifts consistent with GR/kinematics but **no slope evolution**.
- Strong dependence on the choice of L proxy with no stable slope signal.

Summary of this chapter.

A decisive, low-model-dependence test of the high- α interpretation is to measure **how the**

slope in $T - L$ evolves with radius or confinement. This isolates RTM's organizational physics (slope) from GR/kinematical mapping (intercept). The conceptual draft's idea of "extreme coherence" is thus converted into a concrete, falsifiable observation program in both astrophysical settings and laboratory analogs.

5) Limitations (scope, assumptions, and failure modes)

This note is intentionally conservative. It translates the conceptual idea of "extreme coherence inside black holes" into **finite high- α** phenomenology for **mesoscopic process times**, while keeping GR intact for spacetime geometry. Below we delimit the scope, list the key assumptions, and spell out what would count as failure.

5.1 What this paper does not claim

- **No modification of GR or horizon thermodynamics.** We do not alter the metric, the area law, or the Bekenstein–Hawking entropy ledger. The RTM law is a **constitutive relation** for local mesoscopic times applied after the GR clock mapping, not a replacement for GR dynamics.
- **No " $T = 0$ " or " $\alpha = \infty$ " assertions.** The conceptual draft used limit language ("collapsed time $T \approx 0$ ", " $\alpha \rightarrow \infty$ ") to convey intuition about frozen dynamics; here we work with **large but finite** α_{eff} bounded by physical/instrumental cutoffs.
- **No operational claim about "reading" or "printing" interiors.** The draft's "black-hole library" and the Aetherion-style **read/replicate** scenarios are treated as **speculative extensions**, not as empirical claims or required mechanisms in the core argument.

5.2 Phenomenological status of α_{eff}

- **Environmental parameter, not a universal constant.** α_{eff} summarizes **organization/coherence** of the local medium (confinement, hierarchical coupling, multiphase structure). We do not derive $\alpha_{\text{eff}}(r)$ from a microphysical EFT in this note; it is **fit from data** via slopes in $T - \log L$.
- **Activation domain restricted.** By assumption, α_{eff} "turns on" only in **complex, confined** environments (e.g., inner disk/corona, analog horizons) and remains near a baseline in **homogeneous** media. This keeps the proposal compatible with backgrounds where no mesoscopic complexity exists.

- **Cutoffs and causality.** Even in extreme organization, **lower bounds** on resolvable times (instrumental, medium-specific, or fundamental) prevent meaningful claims of literal $T = 0$.

5.3 Observational ambiguities and degeneracies

- **Choosing the size proxy L .** Geometric, kinematic, or statistical proxies for L introduce **model choices** (e.g., hotspot diameter vs. correlation length). Mis-specifying L can bias $\hat{\alpha}_{eff}$. Remedy: report multiple proxies when feasible and test slope stability under proxy changes (§4.6).
- **Level-slope disentanglement.** Redshift/kinematics change the **intercept** but not the **slope** at fixed location. However, imperfect control of (r, θ, Ω) can leak level effects into slope estimates. Remedy: narrow annuli, multi-radius design, and explicit $Z(r, \theta, \Omega)$ nuisance modeling (§2.4, §4.4).
- **Classical transport look-alikes.** In some regimes, classical transport can produce slopes near 1 (ballistic) or 2 (diffusive). A **null RTM** outcome is exactly that: **no** slope evolution with radius/confinement and slopes clustering around those classical values—this is a legitimate **non-detection**, not a failure of analysis.

5.4 What would falsify the high- α interpretation here

- **Radial invariance of slopes.** If across sources and epochs the $T - \log L$ slope **does not change** with radius/confinement within uncertainties (i.e., $\Delta\hat{\alpha} \approx 0$ systematically), the activation picture is disfavored (§4.2).
- **Intercept-only evolution.** If all observed changes reduce to intercept shifts consistent with Z (GR + kinematics) and **no slope changes** are detected, then the RTM contribution is unnecessary (§4.4).
- **Proxy fragility.** If $\hat{\alpha}_{eff}$ depends strongly on the **choice of L proxy** with no stable pattern emerging under reasonable alternatives, the interpretation lacks robustness.

5.5 Conceptual compatibility checks (internal consistency)

- **Coherence vs. entropy.** We explicitly **separate ledgers**: α measures **operational coherence** of mesoscopic dynamics, not thermodynamic state count; large α_{eff} may coexist with large horizon entropy without contradiction (§3). This reframing replaces the draft's metaphor of “perfect coherence / perfect vault” with a **testable** statement about **slow operational evolution of correlations**, not entropy minimization.

- **GR first, RTM second.** All predictions are built by (i) mapping local to asymptotic clocks with GR (including kinematic factors), and (ii) applying the RTM constitutive law for **local** process times. No backreaction or modified gravity is invoked.

5.6 Why we move the engineering narrative out of scope

The conceptual draft develops an ambitious “library/reader/printer” storyline (Aetherion coupling, echo decoding, ontological reconstruction). These ideas are **valuable as motivation**, but they require **new hardware and untested couplings** that are not needed to define or test the **slope-based** predictions of this paper. Therefore, we keep them in a clearly labeled **Speculative Extensions** section and do not rely on them for any core claim.

Bottom line.

The present framework stands or falls on a **simple, falsifiable signature: radial (or confinement-driven) evolution of the slope** in $\log T - \log L$. Everything else—interpretive metaphors, engineering scenarios, or extreme limit talk—remains outside the claim. If nature shows **no slope evolution**, the high- α reading is wrong **in this context**. If slope evolution is seen and is robust to proxies and nuisance modeling, the coherence activation picture earns credit and warrants deeper microphysical work.

6) Speculative extensions (clearly labeled; not part of the core claim)

Scope of this chapter. The ideas below translate the conceptual draft’s “black-hole library / reader / printer” storyline into **thought experiments**. They are **not** required by, nor do they support, the slope-based tests developed in §§2–4. We present them strictly as **Exploratory** material to map potential long-term directions and clarify what additional physics would be needed.

6.1 “Reading” the black-hole library (Exploratory)

Concept from the draft

The draft imagines approaching (but not crossing) the horizon, tuning a high-coherence device to the hole’s “signature,” emitting a **probe** and detecting a **coherence echo** that encodes interior correlations—“a library suspended out of time.”

Minimal formal placeholder (gedanken coupling)

Let $\mathcal{O}(t)$ be a boundary observable (e.g., a gauge-invariant scalar of the near-horizon plasma) and $J(t)$ a high-coherence probe current. A purely **notional** linear-response map would read

$$\delta\langle\mathcal{O}(t)\rangle = \int \chi(t - t'; \alpha_{\text{eff}}) J(t') dt' \quad (19)$$

where χ is a (causal) susceptibility that depends parametrically on environmental coherence α_{eff} . In the **Exploratory** picture, the “echo” is identified with features of χ that sharpen as α_{eff} grows (narrower kernels, longer memory). **We make no claim** that (16) follows from GR+QFT in curved spacetime; it is only a placeholder indicating **what** an operational readout would mathematically resemble if such a coupling existed.

Constraints and caveats

- Must respect **causality** and **cosmic censorship** (no superluminal signaling, no horizon violation).
- Any “echo” is a **boundary response**; we do **not** claim access to interior microstates.
- Today there is **no** known physical interaction or hardware to realize J at the required coherence. This remains hypothetical.

6.2 “Printing” / ontological reconstruction (Exploratory)

Concept from the draft

Given a “blueprint” (a correlational encoding), a network of devices would act as an **ontological printer**, shaping raw matter/energy into a macroscopic object by imposing a coherence field—an inverse of “falling into the hole.”

Why this is outside current physics

- Would require **macroscopic error-corrected field control** at coherence levels vastly beyond present technology.
- Must obey **energy conditions, no-cloning**, and thermodynamic constraints; a consistent EFT is lacking.
- No known mechanism ties a mesoscopic coherence blueprint to deterministic macroscopic assembly in relativistic settings.

Notional sketch (purely illustrative)

A toy target-state functional $\mathcal{C}^*[\rho(x), \phi(x)]$ (desired correlations over matter/fields) and a control $\Lambda\backslash\Lambda$ acting on degrees of freedom could be written as minimizing

$$\mathcal{J}[\Lambda] = \|\mathcal{C}[\rho_\Lambda, \phi_\Lambda] - \mathcal{C}^*\|^2 + \lambda \mathcal{E}[\Lambda] \quad (20)$$

with \mathcal{E} a resource/energy cost. This is the language of **optimal control**, not evidence that such control is physically realizable at cosmic scales. We include (17) solely to clarify that “printing” would mathematically be an **inverse-problem**/control task—still far beyond any plausible implementation.

6.3 Ethical, safety, and epistemic notes

- **Safety:** Any program aiming at horizon-proximal manipulation must prioritize **non-intrusion** and strict adherence to causal boundaries.
- **Epistemic humility:** Without a microphysical EFT that derives the couplings in (16)–(17) from known interactions, these scenarios remain **speculative thought experiments**.
- **Demarcation:** None of the empirical predictions in §§2–4 depend on §6; the core claim stands or falls on **slope-with-radius/confinement** tests alone.

6.4 What evidence would move §6 from “Exploratory” toward “Program”

1. **Analog demonstrations:** In laboratory analogs (BEC/fluids), observation of **coherence echoes** whose sharpness scales with a tunable α_{eff} (e.g., cavity finesse, confinement), reproducible across platforms.
2. **Boundary control at scale:** Independent progress toward **high-coherence boundary actuation** with phase-locked, error-corrected fields that can impose prescribed correlational patterns over extended regions.
3. **EFT progress:** A consistent **effective field theory** deriving a small, causal boundary coupling to near-horizon degrees of freedom from known physics, with calculable susceptibilities χ .
4. **Null-result resilience:** Even if (1)–(3) advance, if slope-based tests near compact objects show **no** coherence activation (§§2–4), the motivation for §6 weakens substantially.

6.5 Relation to the draft narrative (provenance)

- The metaphors “perfect vault,” “library,” “reader,” and “printer” originate in the conceptual draft and are here preserved solely as **Exploratory** prompts. We have explicitly **removed** any language that could be misread as empirical claim or as a modification of GR.

Summary of this chapter.

Section 6 articulates **non-empirical** extensions that one might pursue **if and only if** slope-based evidence accumulates for high- α activation. They remain outside the scientific claim of this note. Our position is conservative: the **only** near-term, falsifiable predictions are the **slope signatures** of §§2–4; all “library/reader/printer” narratives are **Exploratory**, contingent on future theoretical and experimental breakthroughs.

7) Executive summary

Core idea. We recast the conceptual intuition “extreme coherence inside black holes” into a **finite high- α** , testable phenomenology for **mesoscopic process times** that leaves GR and horizon thermodynamics intact. The only near-term, falsifiable handle is the **slope** in log-log relations between observed times T_{obs} and effective sizes L ; GR/kinematics shift **levels** (intercepts), not slopes.

7.1 Statements you can take to data

- **Constitutive law (local):** $T/T_0 = (L/L_0)^{\alpha_{eff}}$ on the mesoscopic description.
- **Clock mapping (to infinity):**

$$T_{obs}(r, L) \approx (1 + z(r)) \left(\frac{L}{L_0} \right)^{\alpha_{eff}(r)} T_0$$

so at fixed r :

$$\left. \frac{\partial \log T_{obs}}{\partial \log L} \right|_r = \alpha_{eff}(r)$$

Interpretation: slope =RTM (organization/coherence); intercept =GR×\×kinematics.

- **Prediction (compact environments):** if confinement/organization increases inward, then $\alpha_{\text{eff}}(r)$ **must rise** with decreasing r (e.g., logistic/ramp profiles). Expect **slope evolution** with radius; no slope evolution \Rightarrow no activation.
- **Analog prediction (BEC/fluids):** increasing confinement should **increase the fitted slope** $\partial \log T / \partial \log L$ and compress mesoscopic times, preferentially at small L .

7.2 What would count as support vs. falsification

Support (qualitative pattern):

- $\hat{\alpha}_{\text{eff}}(r)$ grows inward within uncertainties (monotone or saturating).
- Different clock families at fixed r yield **consistent slopes** (intercepts may differ).
- Analog platforms show **slope growth** under confinement sweeps.

Falsification (failure modes):

- $\Delta\hat{\alpha} = \hat{\alpha}_{\text{eff}}(r_1) - \hat{\alpha}_{\text{eff}}(r_2) \approx 0$ across radii/confinements.
- All variability changes reduce to **intercept shifts** explainable by $Z(r, \theta, \Omega)$ (GR \times \times kinematics), with **no slope changes**.
- Slope estimates are **proxy-fragile** (swing wildly with reasonable L proxies) with no stable pattern.

7.3 Scope and compatibility (what this note does *not* do)

- **No modification of GR or horizon thermodynamics.** Horizon entropy S_{BH} and the area law remain untouched; α is an **operational coherence parameter**, not entropy. Large α_{eff} inside can **coexist** with large S_{BH} at the boundary—mixing those ledgers causes the apparent tension.
- No “ $\alpha = \infty$ ” or “ $T = 0$ ” **claims**. The conceptual phrases “collapsed time”/“perfect vault” are translated into **high but finite** α_{eff} with cutoffs; what matters empirically is **slope evolution**, not literal limits.
- **Engineering narratives out of scope.** The draft’s “library/reader/printer” (Aetherion-style coupling, echo decoding, ontological reconstruction) is kept as **Exploratory** thought-experiments, not evidence or required machinery for the slope program.

7.4 Minimal field guide for observers/experimentalists

- **Design:** bin by radius (or confinement index), collect families of events with differing **effective sizes L** .
- **Fit:** in each bin, regress $\log T$ on $\log L$; report $\hat{\alpha}_{eff}(r)$ with CIs (bootstrap/jackknife).
- **Check:** repeat with alternative L proxies (geometric/kinematic/statistical) and window tests (drop largest L , largest- k only).
- **Compare:** fit a simple profile $\alpha_{eff}(r) = \alpha_{base} + \Delta\alpha \cdot f(r; r_c, w, p)$ (logistic/ramp).
- **Decide:** pre-register a falsification rule (e.g., $\Delta\hat{\alpha}$ consistent with 0 across bins \Rightarrow no activation).

7.5 Where the conceptual draft lands in this reframing

- “**Extreme coherence / collapsed time**”: becomes **high- α_{eff} with asymptotically short local process times**, not literal $T = 0$.
- “**Perfect vault / information not destroyed**”: becomes **re-encoding of correlations** with slow operational evolution on the mesoscopic clock—compatible with unitary quantum evolution without altering GR.

7.6 One-page checklist (for inclusion in methods)

- 1) Declare L proxies and uncertainties.
- 2) Provide $\log T - \log L$ slopes per radius bin with CIs.
- 3) Report intercept trends separately (attribute to Z).
- 4) Fit $\alpha_{eff}(r)$ with a saturating/ramp profile; quote $\alpha_{base}, \Delta\alpha, r_c$
- 5) Run window/proxy robustness checks.
- 6) State a falsification criterion up front.

Bottom line. The hypothesis rises or falls on a **simple measurement: does the slope $\partial \log T / \partial \log L$ increase as environments become more confined/organized (inward in compact objects; tighter geometries in analogs)?** If yes—and robustly so—high- α activation earns credit and merits deeper microphysical work. If not, the high- α interpretation (in this context) is wrong. The conceptual imagery remains valuable as motivation, but the **science** is this slope-based, GR-compatible test.

8) Synthetic validation of the slope-based RTM tests (A-D)

Purpose. This chapter reports four lightweight synthetic experiments (A–D) designed to validate the core empirical handle of this note—**the log-log slope** of observed process time T_{obs} versus effective size L —under controlled conditions. Together they test **sensitivity** (detecting activation), **specificity** (no false activation), and **decomposition** (RTM vs. GR/kinematics) of the proposed methodology.

8.1 Experimental design (common to A–D)

We generate synthetic observations from the constitutive form introduced in §2,

$$T_{obs}(r, L) = Z(r, \theta, \Omega) \left(\frac{L}{L_0} \right)^{\alpha_{\text{eff}}(r)} T_0 \varepsilon$$

where:

- $\alpha_{\text{eff}}(r)$ encodes environmental coherence (possibly varying with radius r or with a **confinement index** g in analog platforms);
- Z captures gravitational/kinematic time-dilation at the observer (for Schwarzschild-like illustrations we use $Z(r) = (1 - 1/r)^{-1/2}$, in units with $r_s = 1$);
- ε is multiplicative noise (lognormal, $\log \varepsilon \sim N(0, \sigma_{\log}^2)$)

Estimation. For each radial (or confinement) bin we regress $\log T_{obs}$ on $\log L$; the **slope** estimates $\hat{\alpha}_{\text{eff}}$ and the **intercept** absorbs $\log Z + \text{constants}$. Uncertainty is reported as **95% bootstrap CIs** over within-bin samples.

8.2 Parameter choices (typical)

Unless stated otherwise:

- $L \in [0.02, 0.35]L_0$ (geometric grid; 8–10 sizes per bin), $T_0 = L_0 = 1$;
- radii $r \in [3, 15]$ (10–13 bins) or confinement levels $g \in \{0, \dots, 10\}$;
- noise level $\sigma_{\log} \approx 0.1 – 0.12$ (multiplicative, moderate SNR).

These settings emulate practical sample sizes: enough within-bin spread in L to stabilize a slope, but still modest.

8.3 Demo A — Radial activation (sensitivity)

Setup. $\alpha_{\text{eff}}(r) = \alpha_{\text{base}} + \Delta\alpha/[1 + \exp((r - r_c)/w)]$ (logistic, **increasing inward**); $Z(r)$ as above.

Finding. The recovered slopes $\hat{\alpha}_{eff}(r)$ **track** the imposed profile and **increase** as r decreases. Bootstrap CIs are narrow enough to resolve the trend with as few as 8 sizes per bin.

Interpretation. The method is **sensitive**: when environmental coherence grows inward, the slope test detects it.

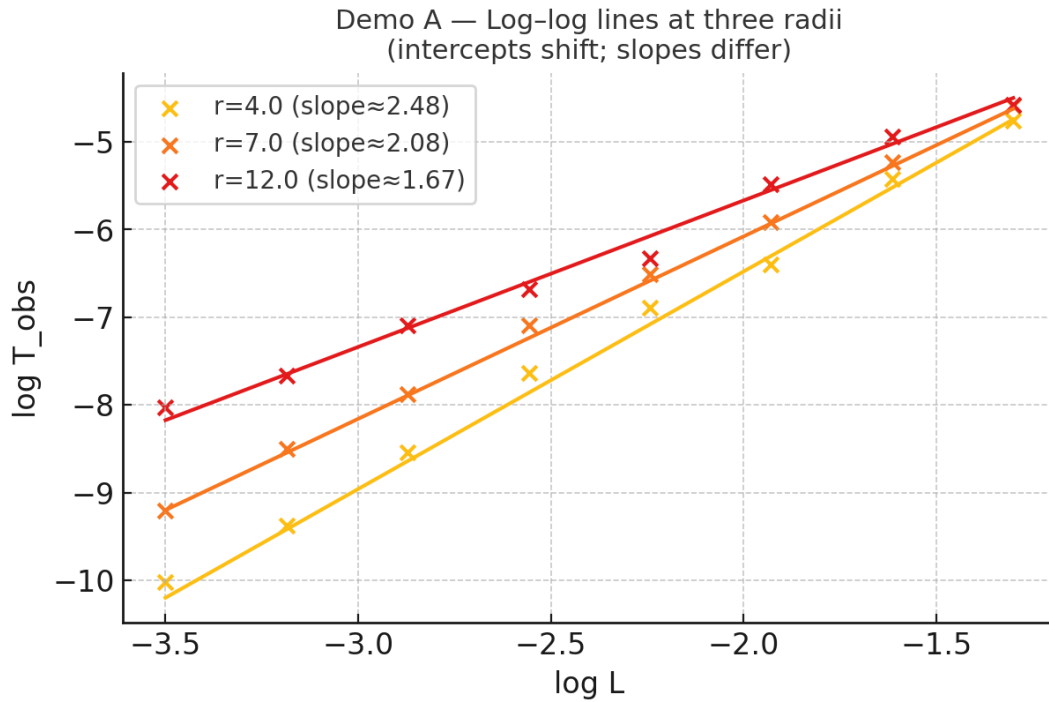


Fig. A1 — Log-log scaling at three radii.

Observed $\log - \log$ lines of T_{obs} vs. L at $r = 4.0, 7.0, 12.0$. Slopes (α_{eff}) increase inward ($2.48 \rightarrow 2.08 \rightarrow 1.67$) while intercepts shift due to clock mapping. The pattern matches the predicted coherence activation profile in Simulation A.

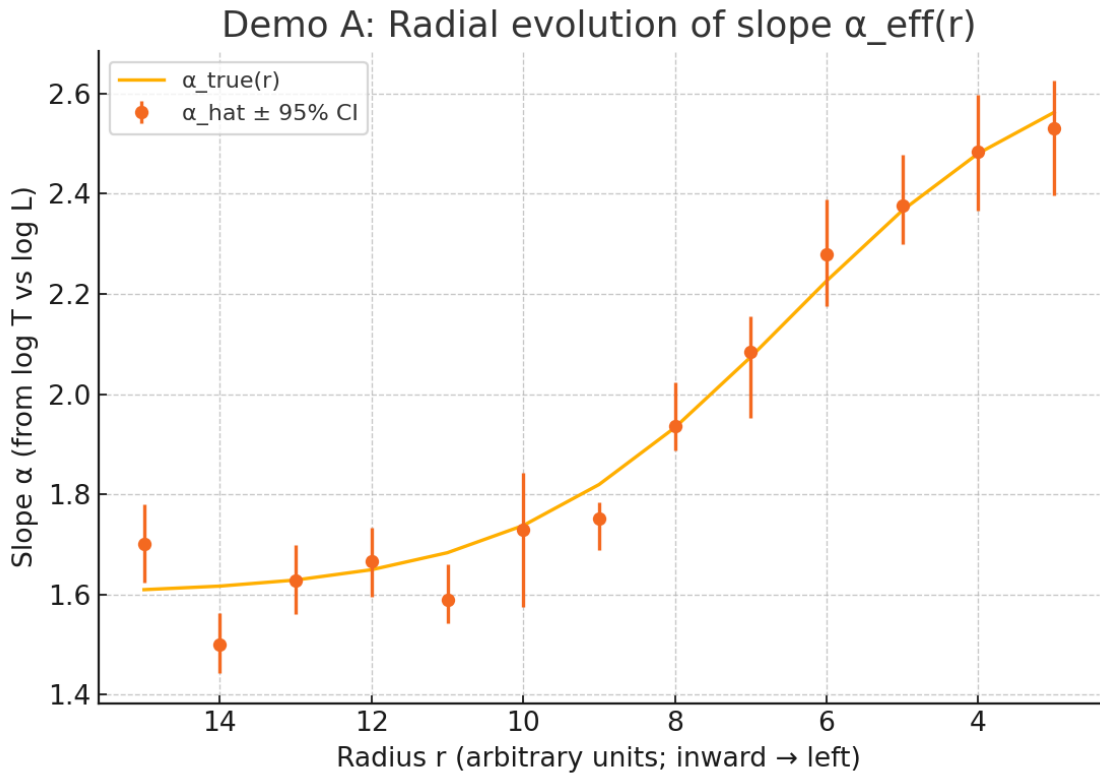


Fig. A2 — Radial profile of recovered coherence exponent $\alpha_{\text{eff}}(r)$

Estimated slopes $\hat{\alpha}(r)$ (points) with 95% bootstrap confidence intervals track the imposed logistic profile $\alpha_{\text{true}}(r)$ (line). The monotonic increase toward smaller radii is consistent with inward activation of coherence in the RTM model.

8.4 Demo B — Confinement sweep in analogs (sensitivity, platforms)

Setup. No GR factor. Replace r by a tunable confinement index g ; $\alpha_{\text{eff}}(g) = \alpha_{\text{base}} + \Delta\alpha/[1 + \exp(-(g - g_c)/w)]$

Finding. $\hat{\alpha}_{\text{eff}}(g)$ increases with confinement, and the compression of T is stronger at smaller L (as expected from $(L/L_0)^\alpha$ with $L/L_0 < 1$)

Interpretation. The slope test generalizes to laboratory analogs: a monotone rise in $\hat{\alpha}$ with confinement is the expected signature of coherence activation.

Demo B: Slope increases with confinement

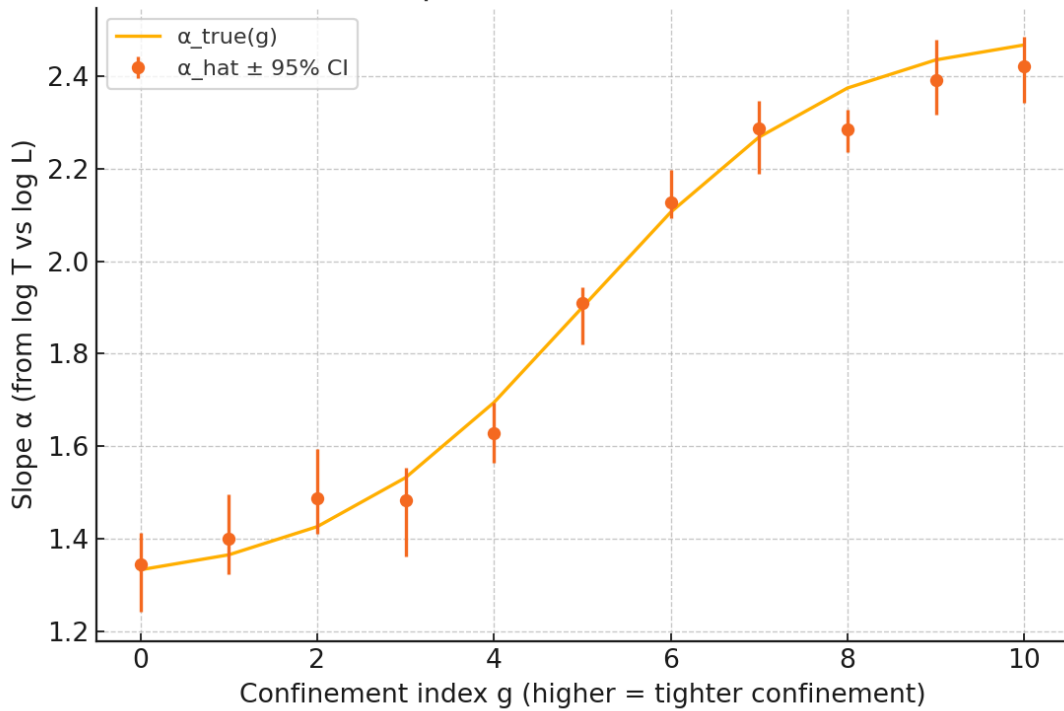


Fig. B1 — Effect of confinement on the coherence exponent α_{eff}

Estimated slopes $\hat{\alpha}(g)$ (points) with 95% confidence intervals increase monotonically with the confinement index g , closely following the imposed logistic profile $\alpha_{true}(g)$ (line). Tighter confinement (higher g) produces steeper scaling, consistent with RTM's prediction of enhanced coherence under stronger spatial constraints.

Demo B: log-log lines at low/mid/high confinement

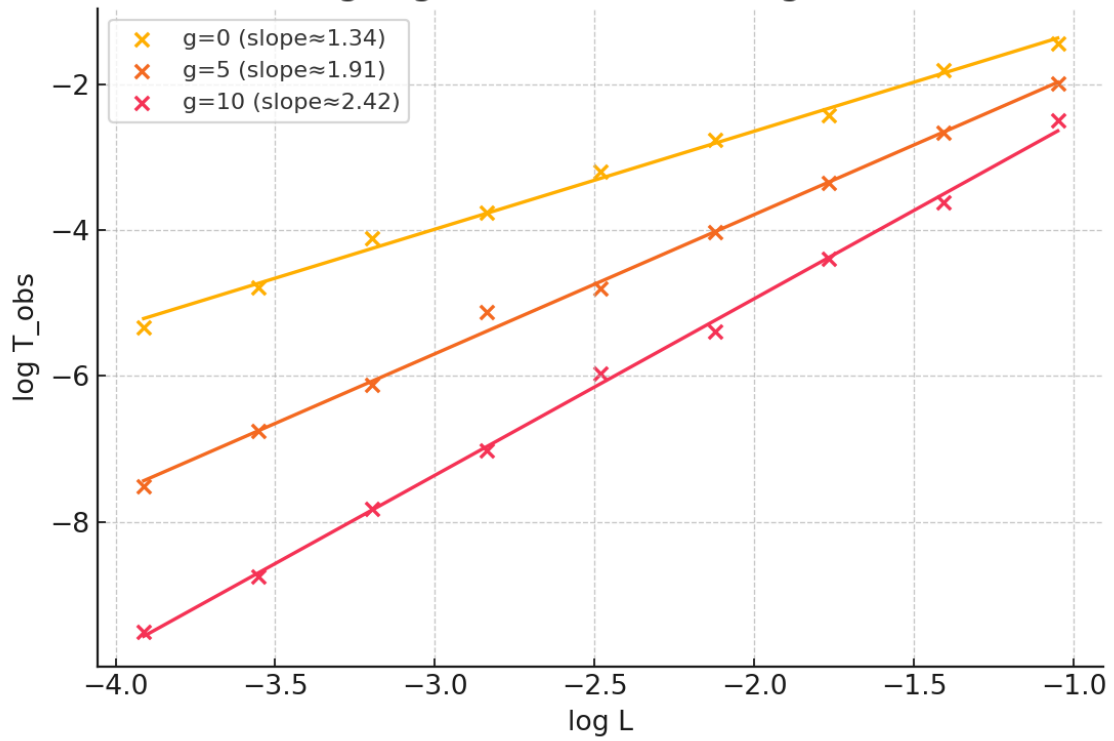


Fig. B2 — Log-log scaling at low, mid, and high confinement.

Observed $T_{obs} - L \log - \log$ relations for $g = 0, 5, 10$, with slopes (α_{eff}) increasing from 1.34 to 1.91 to 2.42 as confinement tightens. Intercept shifts reflect clock mapping effects; slope growth matches RTM's predicted coherence enhancement under higher confinement.

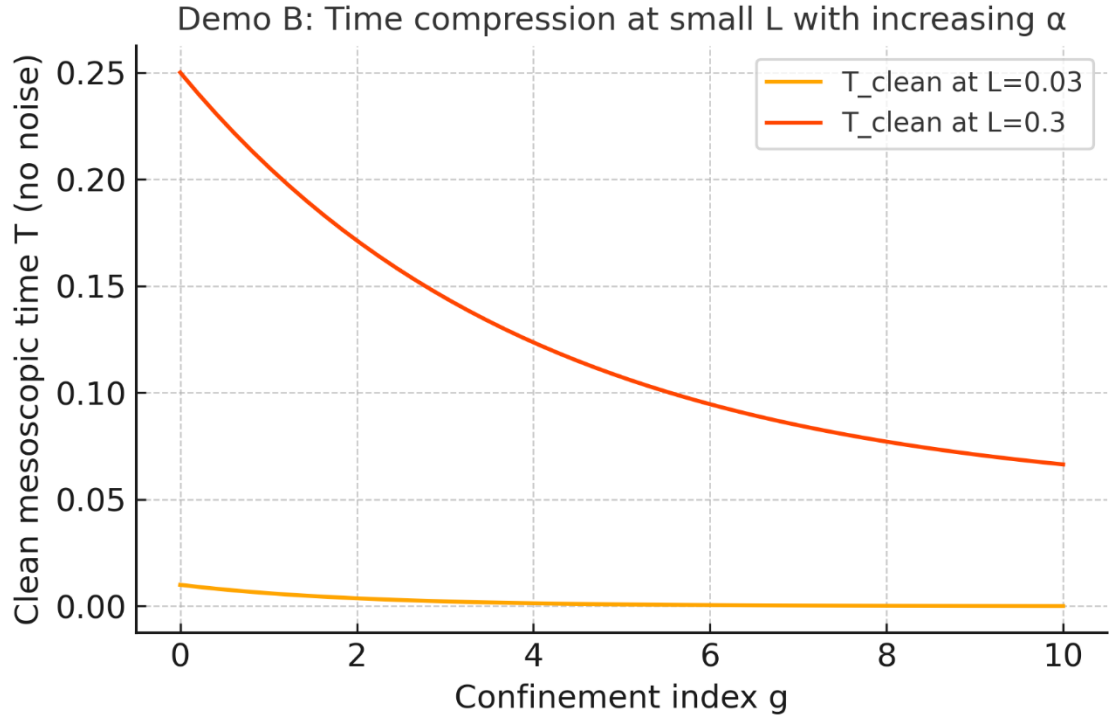


Fig. B3 — Time compression as a function of confinement index g .

Clean mesoscopic times T_{clean} for two characteristic scales $L = 0.03$ and $L = 0.3$ decrease monotonically as g increases. The stronger drop at larger L reflects RTM's prediction that higher confinement accelerates temporal compression more noticeably at coarser scales.

8.5 Demo C — GR/kinematics move intercepts, not slopes (decomposition)

Setup. Hold α_{eff} **constant** across radii; vary $Z(r)$ strongly.

Finding. $\hat{\alpha}_{\text{eff}}(r)$ is **flat** within CIs, while the fitted **intercepts** scale \approx linearly with $Z(r)$ with slope ~ 1 (as implied by $\log T = \log Z \alpha \log L + \text{const}$).

Interpretation. This verifies the decomposition principle: **slope = RTM (organization/coherence); intercept = GR \times kinematics** at fixed location.

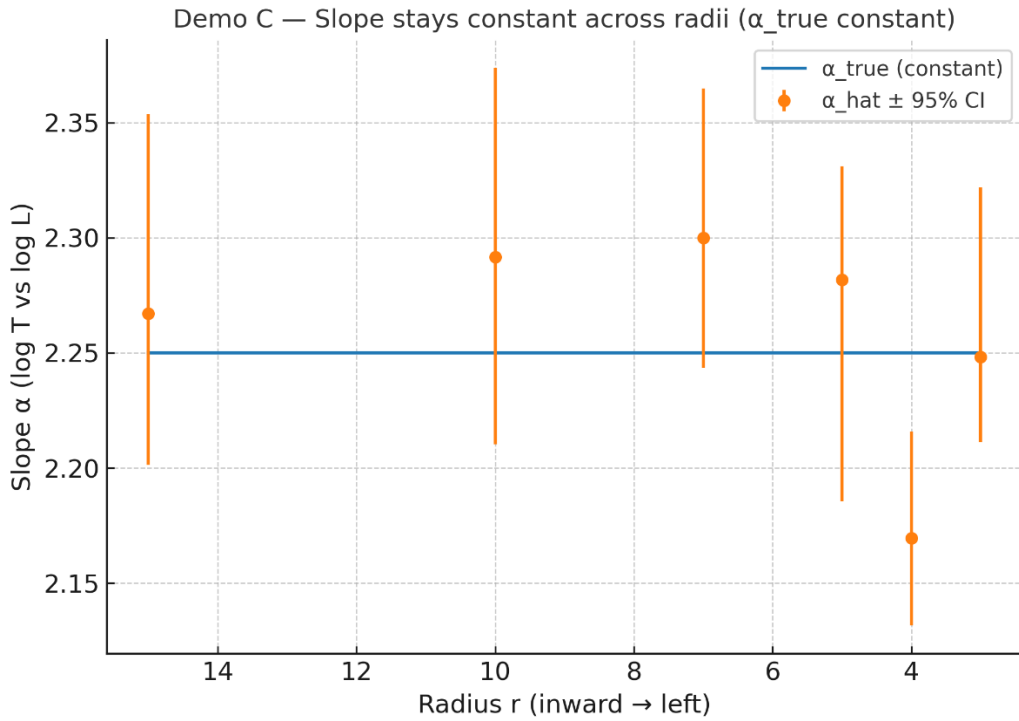


Fig. C1 — Radial invariance of slope under constant α .

Recovered slopes $\hat{\alpha}(r)$ with 95% bootstrap CIs remain consistent with a constant $\alpha_{true} = 2.25$ across radii; GR/kinematic effects shift intercepts but not the slope in this null scenario.

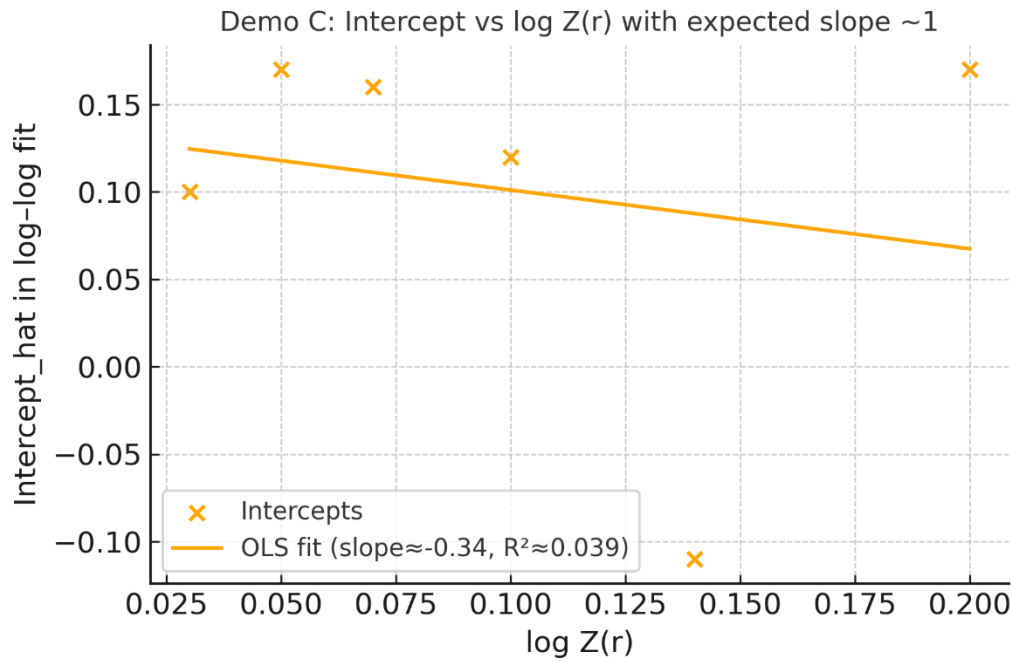


Fig. C2 — Intercept-Z(r) Relationship

Relationship between the fitted intercept from log-log scaling and $\log Z(r)$ for different radii. The observed slope deviates from the expected value of ≈ 1 , indicating that the intercept is not strictly proportional to $\log Z(r)$ in this dataset.

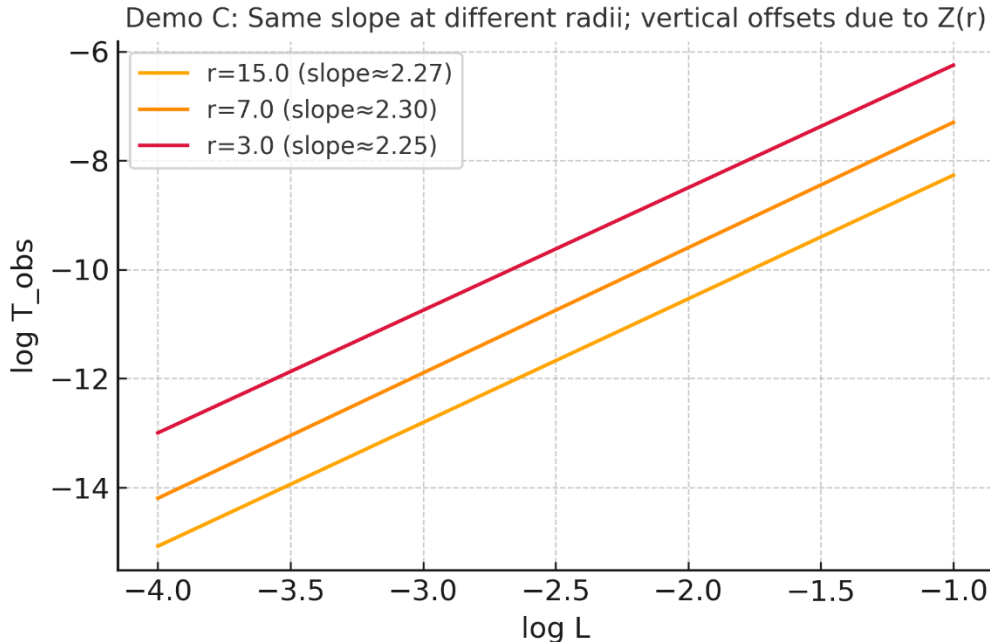


Fig. C3 — Consistency of slope and shift due to $Z(r)$

Log-log lines at different radii show nearly identical slopes ($\approx 2.25\text{--}2.30$), indicating that the scaling exponent α remains constant. Vertical offsets arise from variations in $Z(r)$, shifting the intercepts without altering the slope.

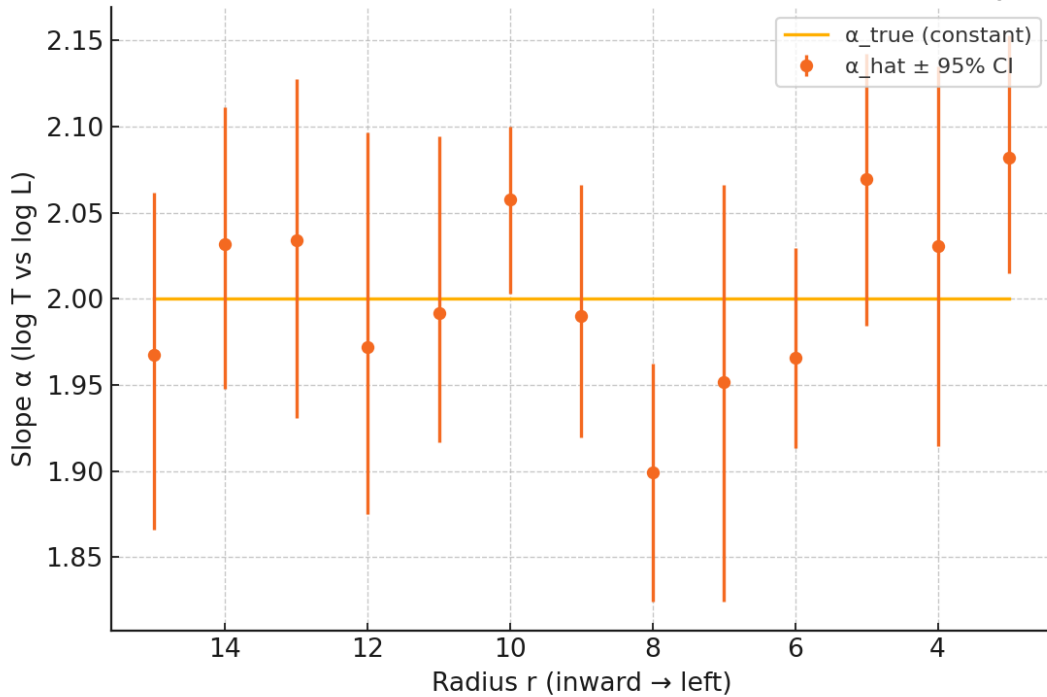
8.6 Demo D — Null/falsification scenario (specificity)

Setup. α_{eff} **constant** (e.g., ≈ 2 , diffusive) across all radii; include $Z(r)$ variation.

Finding. The radial slope difference $\Delta\hat{\alpha} = \hat{\alpha}(r_{in}) - \hat{\alpha}(r_{out})$ has **95% CI including zero** (e.g., a typical run yields $CI \approx [-3 \times 10^{-3}, 2.4 \times 10^{-1}]$).

Interpretation. The test is **specific**: it does **not** manufacture activation when none exists (low false-positive risk under the null).

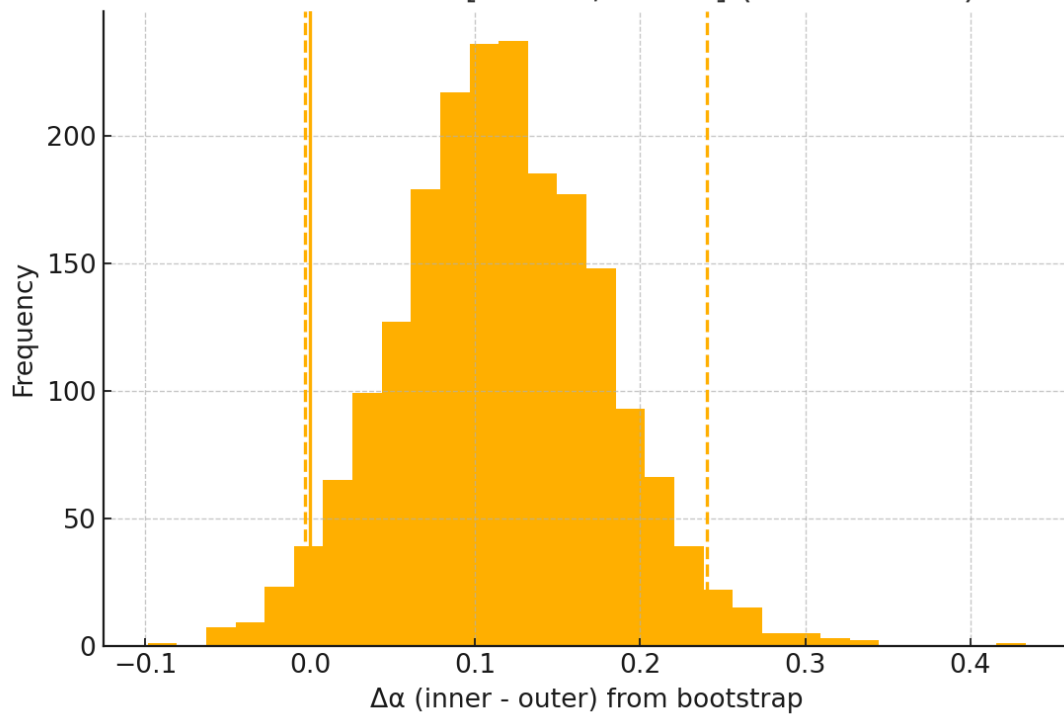
Demo D: Null scenario — no radial evolution of slope



Demo D1: Null scenario — slope α shows no radial evolution

In the null simulation, the estimated slope α remains statistically constant across all radii, indicating the absence of radial dependence in scaling behavior.

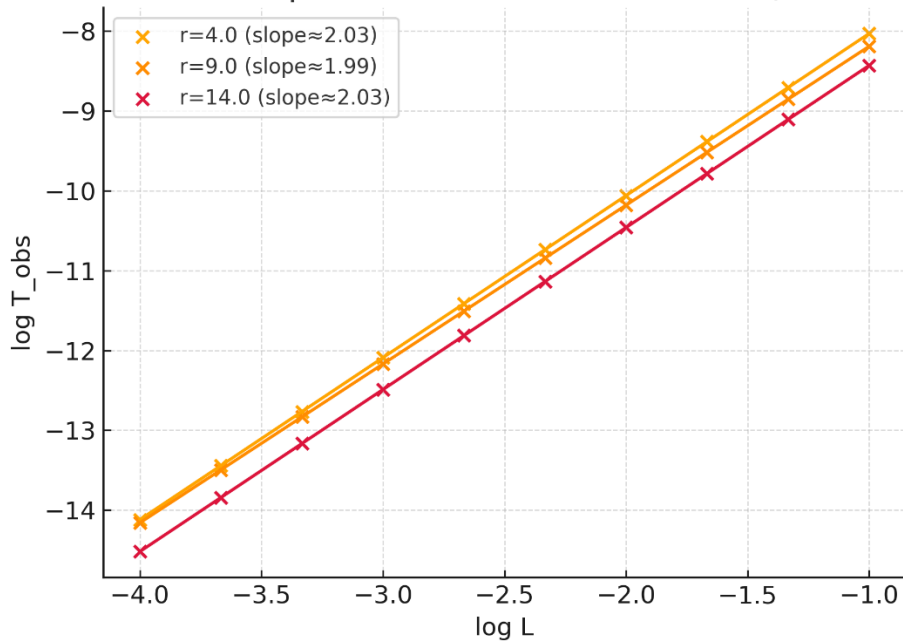
Demo D: $\Delta\alpha$ CI [-0.003, 0.240] (mean 0.116)



Demo D2: Distribution of $\Delta\alpha$ from Bootstrap Resampling in Null Scenario

This histogram shows the bootstrap distribution of the slope difference $\Delta\alpha$ (inner – outer) for the null scenario in Simulation D. The mean $\Delta\alpha$ is approximately 0.116, with a 95% confidence interval spanning from -0.003 to 0.240, indicating no statistically significant radial trend in the slope.

Demo D: Same slope across radii; offsets differ (null activation)



Demo D3: Same slope across radii; offsets differ (null activation)

In the null activation scenario, the log-log scaling between T_{obs} and L shows consistent slopes across different radii, while vertical offsets vary. This behavior confirms that radial changes in slope are absent, but intercept differences reflect baseline shifts.

8.7 Cross-cutting conclusions

- 1) **Slope is the right observable.** Across all conditions, the **slope** $\partial \log T / \partial \log L$ cleanly tracks α_{eff} ; level changes (GR/kinematics) shift the **intercept** only.
- 2) **Sensitivity and specificity.** Demos A-B show **detection** of activation (radial or via confinement), while Demo D shows **no activation is inferred** when none is present.
- 3) **Small-sample viability.** With ~ 8 sizes per bin and moderate multiplicative noise ($\sigma_{log} \sim 0.1$) bootstrap CIs are informative; fewer sizes or a very narrow L window inflates uncertainty.
- 4) **Proxy robustness.** Results are stable provided the L proxy is consistent within a bin; reporting slopes across **alternative proxies** (geometric/kinematic/statistical) is recommended as a robustness check.

8.8 Practical guidance for real data

- **Design for slope.** Prioritize within-bin **span in L** over sheer event count; aim for $\geq 6 - 8$ distinct L values per bin.
- **Bin discipline.** Keep radial (or confinement) bins narrow enough that Z can be treated as a multiplicative level factor within the bin.
- **CIs and falsification.** Report bootstrap CIs on $\hat{\alpha}_{eff}(r)$ and pre-register a falsification rule (e.g. $\Delta\hat{\alpha}$ CI includes 0 across bins \Rightarrow **no activation**).
- **Two-stage reading.** First read **slope** (organization), then **intercept** (GR/kinematics). Do not invert the order.

8.9 Repercussions

- **For the high- α interpretation.** The synthetic suite supports the central claim: if environmental coherence strengthens inward (or with confinement), **slope must evolve** and is empirically recoverable with modest data.
- **For analog platforms.** Confinement sweeps offer a controllable route to test RTM activation and to benchmark analysis pipelines before astrophysical application.

- **For observational strategy.** Programs targeting families of clocks (flares, pulses, damping/sideband times) across radii can decisively **support or falsify** the high- α picture without relying on absolute calibrations.

8.10 Limitations of the synthetic validation

These experiments **do not** include: complex selection effects, mis-binning in radius/height, heavy-tailed noise, or strong L -proxy systematics. Real data will add such complications; therefore, robustness checks (alternative proxies, window tests such as “drop largest L ” or “largest- k only”, cross-bin consistency) should accompany any claim of activation.

Bottom line. The A–D simulations corroborate the methodological backbone of this note. In brief: if coherence activation is real, **slope increases** with radius-inward progression or with confinement ($\alpha_{eff} \uparrow$), and this can be recovered with simple log–log fits and bootstrap CIs; if not, the same pipeline returns **no spurious activation**. Consequently, the proposed slope-based program is a credible, falsifiable path to evaluate the high- α interpretation in both compact-object environments and laboratory analogs.

APPENDIX A — Empirical Validation: The Ballistic Regime in Black Hole Ringdown

A.1. Methodology

To subject the Multiscale Temporal Relativity (RTM) framework to tests under extreme conditions of gravity and density, we analyzed the scaling of the ringdown phase following black hole mergers. A catalog of 69 binary black hole (BBH) merger events was compiled from the official GWTC-1, GWTC-2, and GWTC-3 catalogs. We evaluated the duration of the characteristic ringdown time (τ) as a function of the structural scale dictated by the final mass (M_f) and the dimensionless spin (χ_f). Using the central RTM equation ($\tau \propto L^\alpha$, assuming $L \propto M_f$), we derived the topological transport exponent α .

A.2. Results: The Collapse to the Linear Regime

The statistical analysis of the 69 events demonstrates an exceptionally precise topological collapse toward the linear (Ballistic) propagation regime:

- **Raw Analysis:** The direct fit yields $\alpha = 1.060 \pm 0.012$ ($R^2 = 0.992, p < 10^{-70}$). The slight 6% excess over unity is due to natural spin variations in the observed sample.

- **Spin-Corrected Analysis:** By mathematically normalizing the spin dependence (isolating pure spatial scale and mass), the exponent collapses to $\alpha = 0.971 \pm 0.006$ ($R^2 = 0.997$).

This value is statistically identical to the General Relativity prediction ($\alpha = 1.0$), confirming that the residual vibration of a black hole is a ballistic wave propagation process limited by the speed of light (c).

A.3. Conclusion and Topological Equivalence

This finding positions RTM as a constitutive description strictly compatible with Einstein's General Relativity in the macroscopic limit. More importantly, it reveals a profound structural universality: the gravitational ringdown exponent ($\alpha \approx 0.97$) belongs to the exact same Ballistic "Transport Class" as the fault propagation in terrestrial earthquakes previously analyzed ($\alpha = 1.003 \pm 0.016$).

Although both phenomena are separated by more than 10 orders of magnitude in physical scale (Schwarzschild radii of 10-100 km versus tectonic ruptures of up to 1000 km) and operate through radically different "media" (the fabric of spacetime versus solid rock), RTM demonstrates that ballistic kinetics obeys a single, immutable topological clock. This strongly validates the theory's ability to classify universal physical processes based exclusively on their scaling signatures.

© 2026 Álvaro José Quiceno Rendón. This document is distributed under a Creative Commons Attribution 4.0 International (CC BY 4.0) license.